WORLD JOURNAL OF PHARMACEUTICAL RESEARCH
SJIF Impact Factor 8.084
Volume 11, Issue 1, 1836-1858. Research Article ISSN 2277– 7105

LIGAND DECORATED NANOPARTICLES OF COLCHICINE FOR TARGETING BREAST CANCER CELLS

Sandhya, Devender Chauhan, Dr. Dinesh Kaushik*

Hindu College of Pharmacy, Sonipat.

Article Received on
18 Nov. 2021,

Revised on 08 Dec. 2021,
Accepted on 28 Dec. 2021

DOI: 10.20959/wjpr20221-22762

***Corresponding Author**
Dr. Dinesh Kaushik
Hindu College of Pharmacy,
Sonipat.

ABSTRACT

The field of nanotechnology has rapidly evolved as evidenced by the fact that there are more than 150 ongoing clinical trials investigating the efficacy of nanotechnology based drug delivery carriers targeting cancer. Breast cancer refers to the erratic growth and proliferation of cells that originate in the breast tissue. Anticancer drugs, which have been developed from natural products are Colchicine. Colchicine one such natural alkaloid is colchicine, extracted from the stem of saffron meadow (*Colchicine autumnale*). Folate conjugated gelatin was synthesized using covalent coupling technique. Physicochemical characterization of nanoparticles are spectra (FTIR), Differential scanning calorimetry (DSC),Transmission electron microscopy (TEM), Powder X-ray diffraction (PXRAD), Particle size, Encapsulation efficiency and drug loading capacity, In vitro drug release, Cytotoxicity assay, Cellular uptake in cancer cells. We have synthesized ligand decorated nanoparticles using folic acid and gelatin for targeting breast cancer cells. *In vitro* cytotoxicity and cellular uptake study confirmed that CLC-FA-GNs with greater efficacy compared with CLC alone and CLC-GNs may potentially be used for targeting breast cancer cells.

KEYWORDS: Nanoparticles, Gelatin, Colchicine.

INTRODUCTION

Nanotechnology offers drugs in the nanometer size range which enhances the performance in a variety of dosage forms. Various advantages of nano sizing are decreased patient-to-patient variability, Enhanced solubility and increased oral bioavailability. The field of nanotechnology has rapidly evolved as evidenced by the fact that there are more than 150

ongoing clinical trials investigating the efficacy of nanotechnology based drug delivery carriers targeting cancer.[1]

Classification of nanoparticles

Nanoparticles are broadly classified in to three classifications

- **One dimension nanoparticles**

One dimensional system (thin film or manufactured surfaces) has been used for decades. Thin films (sizes 1–100 nm) or monolayer is now common place in the field of solar cells offering, different technological applications, such as chemical land biological sensors, information storage systems, magneto-optic and optical device, fiber-optic systems.

- **Two dimension nanoparticles**

Carbon annotates

- **Three dimension nanoparticles**

Dendrimers, Quantum Dots, Fullerenes (Carbon 60), (QDs)

Nanoparticles prepared by different methods

Solvent evaporation method

Solvent evaporation method is one of the most frequently used methods for the preparation of nanoparticles. This method involves two steps (first is emulsification of the polymer solution into an aqueous phase and second is evaporation of polymer solvent, inducing polymer precipitation as nanospheres).

Spontaneous emulsification or solvent diffusion method

This method is developed from solvent evaporation method, in which the water miscible solvent along with a small amount of the organic solvent (water immiscible) is used as an oil phase. During the spontaneous diffusion of solvents between the two phases an interfacial turbulence is generated which may ultimately leads to the formation of small particles.

Double Emulsion and Evaporation method

Most of the emulsion and evaporation based methods suffer from the limitation of poor entrapment of hydrophilic drugs. Therefore to encapsulate hydrophilic drug the double emulsion technique is employed, which involves the addition of aqueous drug solutions to organic polymer solution under vigorous stirring to form w/o emulsions. This w/o emulsion is added into second aqueous phase with continuous stirring to form the w/o/w emulsion. The emulsion then subjected to solvent removal by evaporation and nano particles can be isolated

by centrifugation at high speed. The formed nanoparticles must be thoroughly washed before lyophilisation. In this method the amount of hydrophilic drug to be incorporated, the concentration of stabilizer used, the polymer concentration, the volume of aqueous phase are the variables that affect the characterization of nanoparticles.

Salting out method

Method involves the separation of a water-miscible solvent from aqueous solution via a salting-out effect. It's based on the on the separation of a water miscible solvent from aqueous solution via a salting-out effect. During the initial process polymer and drug are dissolved in a solvent which is subsequently emulsified into an aqueous gel containing the salting out agent and a colloidal stabilizer.

Emulsions-Diffusion method

The encapsulating polymer is dissolved in a partially water-miscible solvent (such as propylene carbonate, benzyl alcohol), and saturated with water to ensure the initial thermodynamic equilibrium of both liquids. Subsequently, the polymer-water saturated solvent phase is emulsified in an aqueous solution containing stabilizer, leading to solvent diffusion to the external phase and the formation of nanospheres or nanocapsules, according to the oil-to-polymer ratio. Finally, the solvent is eliminated by evaporation or filtration, according to its boiling point. This technique presents several advantages, such as high encapsulation efficiencies (generally 70 %), no need for homogenization, high batch-to-batch reproducibility, ease of scaleup, simplicity, and narrow size distribution.[2,3]

C**olchicine:** One such natural alkaloid is colchicine, extracted from the stem of saffron meadow (*Colchicine autumnale*). The colchicine binding site on tubulin protein is well characterized. Colchicine is a protoptype class of antimitotic agent known as spindle poisons. It binds at the interphase of α and β subunits of the tubulin heterodimer.

Gelatin: Gelatin is a translucent, colorless, brittle, flavorless food derived from collagen obtained from various animal body parts. It is commonly used as a gelling agent in food, pharmaceutical drugs, vitamin capsules, photography, and cosmetic manufacturing.[7]

OBJECTIVE

The research work is to prepare nanoparticles of colchicine with gelatin to achieve the following objectives are:

- To formulate and evaluate gelatin nanoparticles containing colchicine for targeting breast cancer cells.
- To study the *in-vitro* release of nanoparticles of colchicine.

MATERIALS AND METHODS

Materials

Table 4.1: List of Reagents and Chemicals.

S. No.	Materials	Company
1	Colchicine	Loba chemie
2	Gelatin	Qualigens/Fisher Scientific
3	Folic acid	CPH
4	Acetone	Rankem
5	Methanol	Rankem
6	Gluteraldehyde	Loba chemie

Methods

Synthesis of folate conjugated gelatin

Folate conjugated gelatin was synthesized using covalent coupling technique. Briefly 20mm of folic acid (FA) was added to a mixture of 1-(3-dimethylaminopropyl)-3-ethyl carbodiimide hydrochloride (EDAC.HCl) and N-hydroxy succinimide (NHS) (40mm:40mm) prepared in 100 mL of methanol. The mixture was stir for 6 hrs. After stirring to add 20mm gelatin. The process was give folic acid conjugated gelatin. When gelatin was combined with folic acid in presence of EDAC (which is used for amine coupling reaction) utilized carboxylic group from folic acid and NH group from gelatin during the reaction. And this formed the folate-CONH-gelatin.

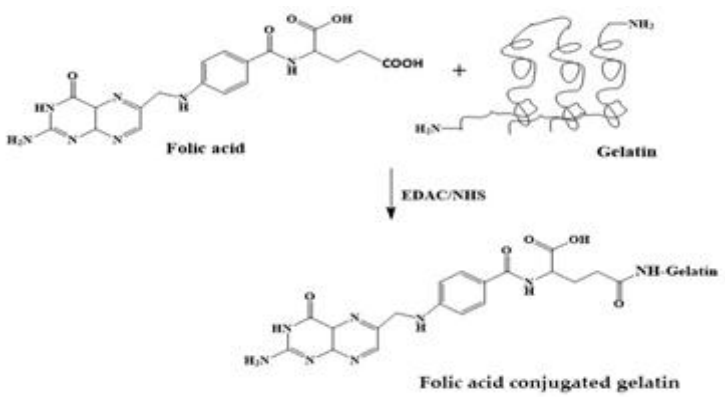

Preparation of gelatin nanopartilces

Colchicine loaded gelatin nanoparticles (CLC-GNs) were prepared by previously optimized two-step desolvation method. Briefly, 25 mL of gelatin solution (5% w/v) was prepared at room temperature and desolvated using 25 mL of acetone to precipitate high molecular weight gelatin. The solution was then kept for sedimentation. Subsequently, supernatant liquid was discarded and the sediment was re-dissolved in 25 mL of distilled water containing 1 mg/mL of colchicine at pH ~ 2.5. Acetone was again added drop-wise to form colchicine loaded gelatin nanoparticles (CLC-GNs). Nanoparticles were further cross-linked with 500 mL of glutaraldehyde. The excess of glutaraldehyde was neutralized by adding 500 mg of glycine. Purification was done by centrifugation at 40,000 rpm in an ultracentrifuge (Thermo Scientific, Sorvall Ultra Centrifuge). The resultant pellet of nanoparticles was lyophilized (Lab India, Thane, India) in the presence of 5% w/v trehalose (lyoprotectant) to produce CLC-GNs.

Methodology

Analytical estimation of CLC

10.0 mg of standard CLC was dissolved in methanol to make 10 ml stock solution, of which different volumes were used to prepare the working solution and absorbance was read at 350 nm using UV-VIS spectrophotometer (Shimadzu, Japan).

Physicochemical characterization

Fourier-transform infrared spectra (FTIR)

Fourier transforms infrared (FTIR) spectroscopy to analyze the chemical compatibility between the drug and the polymer. The spectrum was recorded for CLC, GNs, physical mixture of CLC and GNs and CLC-GNs using a Spectrum BX (Perkin Elmer) infrared spectrophotometer. Pellets of samples were prepared with KBr (2 mg sample in200 mg KBr) using a hydrostatic press at a force of 40 psi for 4 min. The scanning range was 4000–400 cm^{-1} and the resolution was 4 cm^{-1}.

Powder X-ray diffraction pattern (PXRD)

The crystal structure of the drug in the nanomatrix system, powder X-ray diffraction (PXRD) patterns of CLC, GN, physical mixture of CLC and GN, folate conjugate GNs and GN-CLC were recorded at room temperature using X'pert PRO,PANalytical with Ni- filtered CuKα radiation operated at a voltage of 45 kV, cuurent 40 mA, 1 min^{-} scanning speed, and 10 - 15 diffraction anlge (2θ) range.

Transmission electron microscopy (TEM)

The surface morphology of nanoparticles was determined using a transmission electron microscope (Philips Morgagni 268, FEI Electron Optics, Eindhoven, and the Netherlands) at a constant voltage of 80 kV. A drop of aqueous dispersion of the nanoparticles was placed on a carbon- coated copper grid. Subsequently, the grid was allowed to dry in air for 10 min and loaded onto the microscope. A scale bar of 200 nm was used to capture the photomicrographic.

Differential scanning calorimetry (DSC)

Thermal behavior of CLC, Gelatin, physical mixture of CLC and gelatin and CLC-Gelatin nanoparicles was examined using a diffential scanning calorimetry (DSC) Q200 V23.10 Build 79 (Universal V 4.4A TA Instrument) thermal analyzer.

Particle size

Particle size analyzer (Malvern Instruments, Worcestershire, UK) for determination of nanoparticles size and surface charge. Briefly, 100 µl of the nanoparticles susupension was added to 5 ml of phosphate buffer saline (pH 7.4), and the mean particle size and polydispersity index were determined. All measurements were carried out at 25º C in the same onoic concentration at a light scattering angle of 90º.

Encapsulation Efficiency and Drug loading capacity

The encapsulation efficiency of all the formulations was calculated by dispersing the nanoparticles (50 mg) in 50 ml of 0.02N hydrochloric acid, followed by warming for a few minutes, incubation for 48 h, and centrifugation at 8000g. The supernatant was filtered through a 0.2 mm membrane filter and an aliquot of the filtrate was diluted appropriately with the respective solvent system. The concentration of Nos in all the formulations was determined by measuring the optical density at 350 nm using a UV–Visible Spectrophotometer (Shimadzu) 158. The encapsulation efficiency and drug-loading capacity were calculatedusing the following formula:

$$\text{Encapsulation efficiency} = \frac{\text{Amount of drug entrapped}}{\text{Amount of drug added}} \times 100$$

$$\text{Drug loading capacity} = \frac{\text{Amount of drug present}}{\text{Practical yield of nanoparticles}}$$

In-vitro drug release profile

The in-vitro drug release of CLC from nanovectors was carried out at 37±11ºC at slightly acidic pH (7.4) in the dark using the dynamic dialysis technique, a method for quantification of drug transport across a dialysis membrane (159). Briefly, a suspension of GN-CLC (5mg dispersed in 1ml normal saline) was dialyzed against 100ml of phosphate buffer solution, respectively. At a predetermined time interval, 1 ml of the dissolution medium was withdrawn and replaced with fresh solvent to mimic infinite sink conditions. Absorbance of the withdrawn sample solutions was measured at 350 nm using a UV-visible spectrophotometer (Shimadzu) and concentration of CLC was calculated using a standard calibration curve.

Cytotoxicity assay

The MTT assay was used to evaluate the proliferative capacity of cells treated with various nanoparticle formulations. Briefly, 3×10^3 MDA-MB-231 cells per well were seeded in a 96-well format. After 24 h of incubation, cells were treated with a gradient concentration of CLC, CLC-GN and respective blank formulations. After 72 h of drug incubation, the spent medium was removed and the wells were washed twice with PBS. A final concentration of 5 mg/ml MTT was added to each well and cells were incubated at 371ºC in the dark for 4 h. The formazan product was dissolved in 100% dimethyl sulfoxide after removing the medium from each well. The absorbance was measured at 350nm using a plate reader (Tecan).

Cellular uptake assay

Both quantitative and qualitative cellular uptake assays were performed by fluorometry. In brief, MDA-MB-231 were plated in Lab-Tek II Chamber SlideTM System (Nalge Nune, USA) at a density of 5×10^3 cells per chamber. Dosing solutions of FITC-labeled CLC-GNs and optimized CLC-GNs-FA (equivalent to 10 to 70 mM concentration of cisplatin) were prepared using PBS (pH~7.4) and diluted with FA- free-DMEM. Cell monolayers were rinsed thrice and pre-incubated with 1 mL of FA-free-DMEM at 37ºC for 1 h. Uptake was commenced when 1 mL of specified dosing solution was exchanged with culture medium, followed by incubation of the cells at 37ºC for 24 h. The experiment was terminated by washing the cell monolayer thrice with ice-cold PBS (pH~7.4) and cells were lysed with 1 mL of 0.5% Triton X-100. Cell associated FITC was quantified by analyzing the cell lysate in a fluorometer (Spectra Fluor, Tecan, Switzerland, λ_{lexe} ~485 nm, λ_{lemi} ~535 nm). The protein content of the cell lysate was measured using the BCA protein assay kit. After 24 h

incubation period, the medium was removed and plates were washed thrice with sterile PBS (pH~7.4). After the final wash, the cells were fixed with 4% paraformaldehyde and individual cover slips were mounted on clean glass slides with fluoromount-G mounting medium (Southern Biotechnology, Birmingham, AL). The slides were viewed under a confocal laser-scanning microscope (λ_{lexe} ~485 nm, λ_{lemi} ~535 nm). DAPI (4,6-diamidino-2-pheny- lindole) was used for nucleus staining.

Statistical analysis

The statistical analysis was carried out using one-way and two-way analysis of variance tests. All results were expressed as mean ±SD for n value of at least 3. A probability (P) value of less than 0.05 was considered statistically significant.

RESULTS AND DISCUSSION

Analytical estimation of colchicine

10.0 mg of standard CLC was dissolved in methanol to make 10 ml stock solution, of which different volumes were used to prepare the working solution and absorbance was read at 350 nm using UV-VIS spectrophotometer. From this solution of conc. 5µg/ml to 40µg/ml were prepared.

Table 5.1: Estimation of colchicine in methanol using UV-VIS spectrophotometer.

S. no.	Concentration (µg/mL)	Absorbance (nm)
1	0	0
2	5	0.07
3	10	0.138
4	15	0.183
5	20	0.25
6	25	0.31
7	30	0.37
8	35	0.46
9	40	0.51

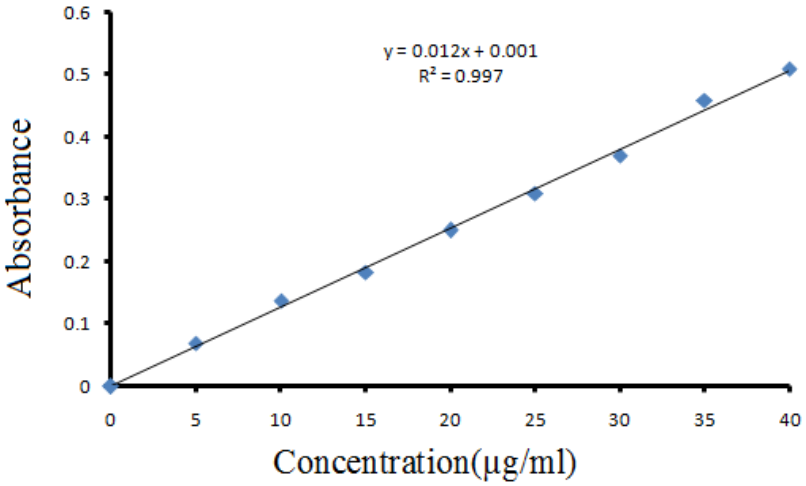

Figure 5.1: Standard calibration curve of colchicine at 350 nm.

Preparation of gelatin nanoparticles

Colchicine loaded gelatin nanoparticles (CLC-GNs) were prepared by optimized two-step desolvation method. Trehalose was used as a lyoprotectant, which prevented aggregation of nano-particles and reduced mechanical stress during freezing and drying processes. Subsequently, folic acid (FA-COOH) was anchored onto the surface of drug loaded nanoparticles (–NH2) using conjugation chemistry. This conjugation reaction yielded a stable amide bond with FA. The FA content was measured to be 6.3, 15.1, 25.4 and 25.9 n.mol/mg of CLC-GNs at the incubation period of 3, 6, 12 and 24 h, respectively. The CLC-GNs-FA nanoformulation with 25.9 n.mol FA and modification of 32% amine groups (preferably lysine) was designated as optimized nanoformulation.

Physiological characterization

Fourier-transform infrared spectra (FTIR)

We characterized the nanoparticles by various spectroscopy techniques. FT-IR spectra were recoreded to analyze the structure of new chemical linkage formed. The FTIR spectrum peaks of CLC, gelatin, folic acid, physical mixture of CLC and GN, are shown in Table 6. The FTIR spectrum of CLC shows a characteristics peak at 3452 cm^{-1}, indicating the presence of N-H stretching in secondary amide. Others of CLC observed are 2892 cm^{-1} for C-H stretching, 1012 cm^{-1} for C-C stretching, 1456 $cm^{-1}$for C==C stretching, and 3517 and 1559 cm^{-1} for N-H bending. The spectrum of GN shows peak at 3390 and 3478 cm^{-1} for N-H stretching, 1011 cm^{-1} for C-C stretching, 2976 cm^{-1} for C-H stretching,1632 cm^{-1} for C=C stretching. The FTIR spectrum of folic acid shows a peak at 3545 cm^{-1} for N-H stretching, 1693 cm^{-1} for O-H stretching and 766 cm^{-1} for C-C def.

Table 5.2: FTIR spectrum of CLC, GN, and physical mixture of CLC, GN and gelatin folate conjugate.

Sample	Infrared peaks (cm^{-1})	Functional groups
CLC	3452	(N-H stretching)
	2892	(C-H stretching)
	1012	(C-C stretching)
	1456	(C=C stretching)
	3517; 1559	(N-H bending)
GN	3390;3478	(N-H stretching)
	1011	(C-C stretching)
	2976	(C-H stretching)
	1632	(C=C stretching)
	2202	(C≡C stretching)
	3124	(≡C-H stretching)
Folic acid	3545	(N-H stretching)
	2925	(C-H stretching)
	1693	(O-H stretching)
	1485	(C-H def)
	818	(C-H def)
	766	(C-C def)
Physical mixture of CLC and GN	3615;3648	(O-H stretching)
	3391	(N-H stretching)
	2813	(C-H stretching)
	695	(C-C bending)

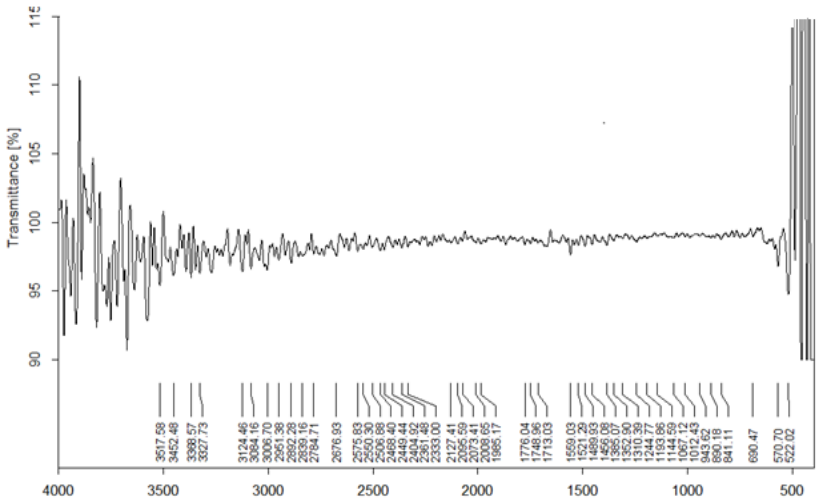

Fig. 5.2: FT-IR spectra of colchicine.

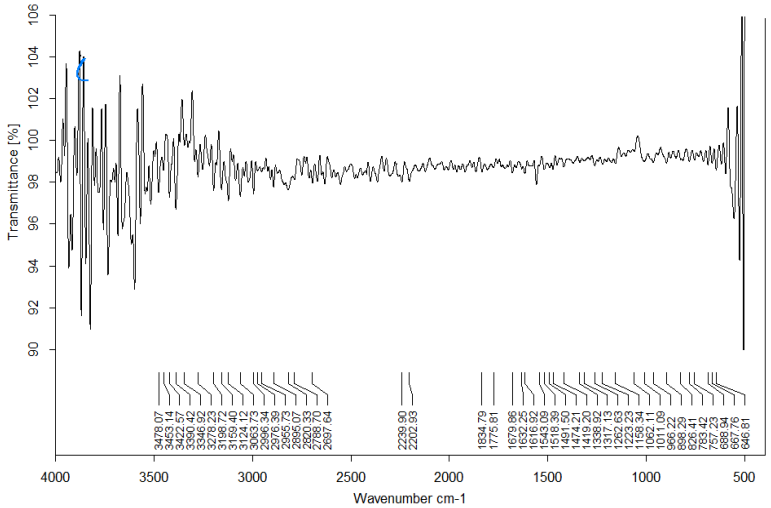

Fig. 5.3: FT-IR spectra of gelatin.

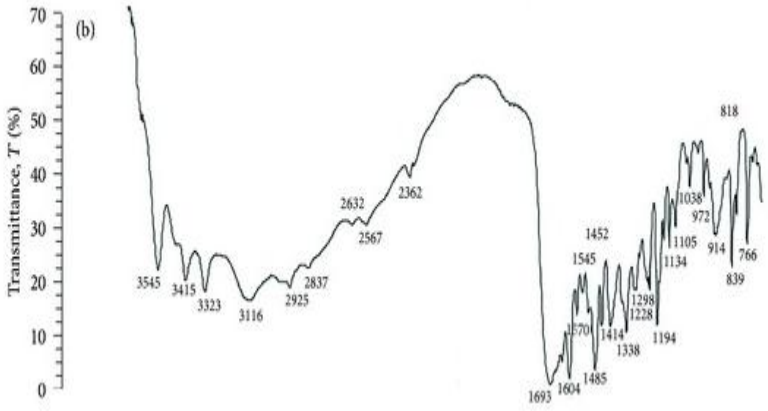

`Figure 5.4: FT-IR spectra of folic acid.

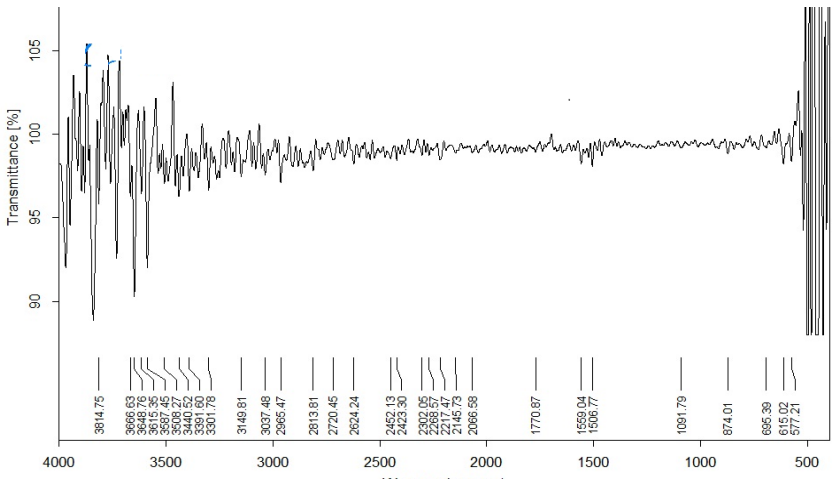

Fig. 5.4: FT-IR spectra of physical mixture of CLC and gelatin.

Powder X-ray diffraction pattern (PXRD)

We attempted to define the crystalline structure of the drug in the folate conjugates using PXRD technique. The PXRD pattern of CLC showed peaks that were intense and sharp

indicating its crystalline structure. The gelatin showed sharp peak. The folic acid also showed the sharp peak and form a crystalline structure. The physical mixture of CLC, gelatin and folic acid showed sharp peaks with maximum intensities. Though this signifies crystalline structure of all mixtures. Finally, the folate conjugates of CLC with gelatin showed undefined, broad peaks of diminished intensities. This suggested that CLC is present in the high energetic amorphous state in CLC-GN-folate conjugates, which is more wettable than crystalline state.

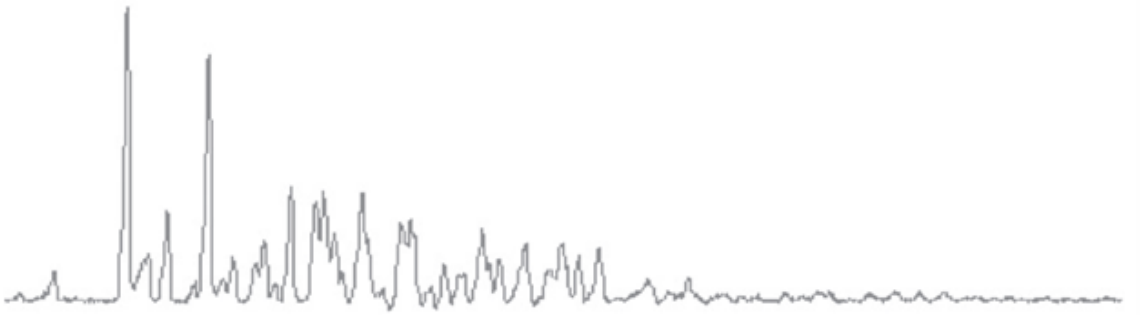

(A)

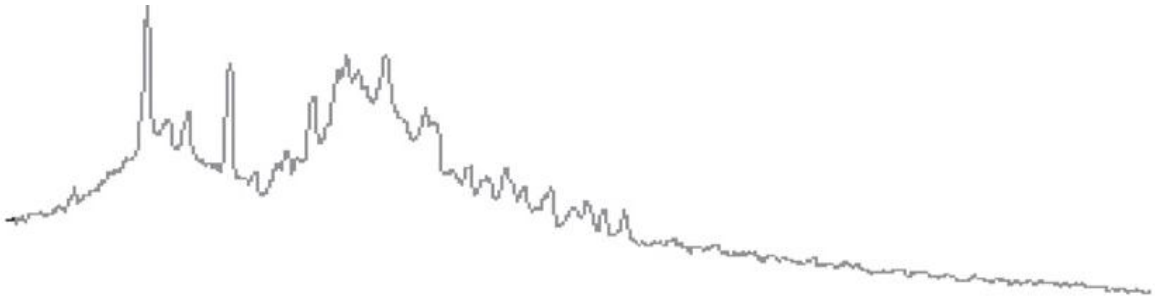

(B)

(C)

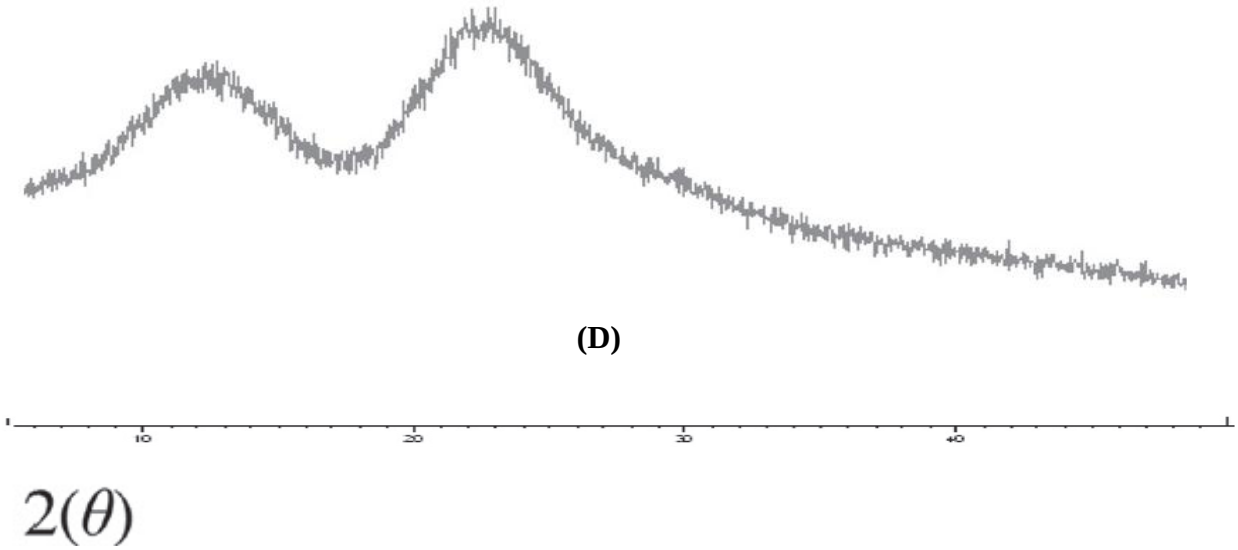

(D)

Figure 5.5: PXRD of (A) Colchicine, (B) Gelatin, (C) Colchicine loaded gelatin nanoparticles, (D) Folic acid conjugated colchicine loaded gelatin nanoparticles.

Transmission electron microscopy (TEM)

The TEM micrographs of lyophilized CLC loaded GN nanoparticles and folic acid conjugated CLC loaded GN nanoparticles suugested that the nanoparticles were smooth and spherical in shape. The photomicrographs indicated that centrifugal force and freeze-drying factors did not affect nanoparticles texture. The most peripheral human tumor vessels have a permeability cut-off of less than 100 nm.The CLC loaded GN nanoparticles and folic acid conjugated CLC loaded GN nanoparticles, therefore, may provide an effective means of NOS delivery to solid tumors after intravenous or intratumoral administration of the formulations in future in-vivo studies.

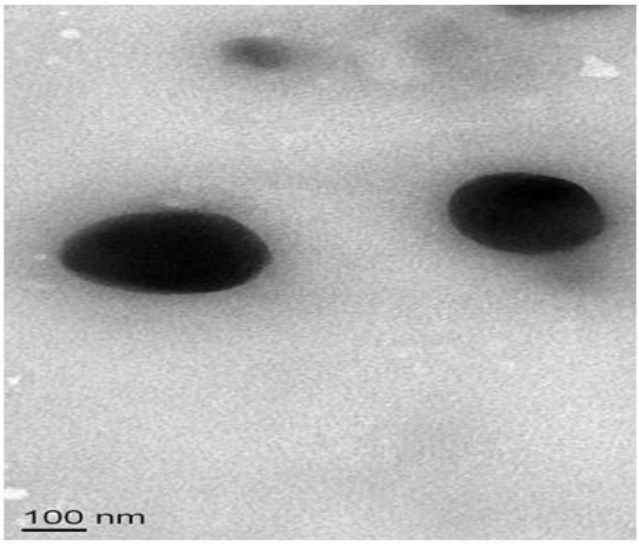

(A)

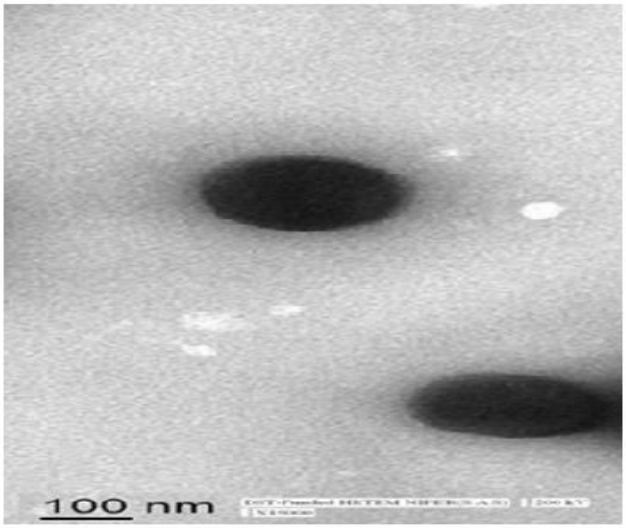

(B)

Figure 5.6: (A) TEM of CLC loaded gelatin nanoparticles and (B) Folic acid conjugated CLC loaded gelatin nanoparticles.

Differential scanning calorimetry (DSC)

The thermal behavior of the nanoparticles was compared to that of the original species by DSC measurements. DSC curve of CLC showed a sharp endothermic peak near 155ºC that is indicative of its melting temperature. DSC curve of gelatin exhibit endothermic peak at 60ºC. DSC curve of folic acid also endothermic peak at 252ºC. Finally, the formation of gelatin-folate conjugates and the peak at 156ºC CLC-GN-folate conjugates starts to decompose at this temperature. Hence, DSC analysis confirmed the formation of CLC-GN- folate conjugate in solid state.

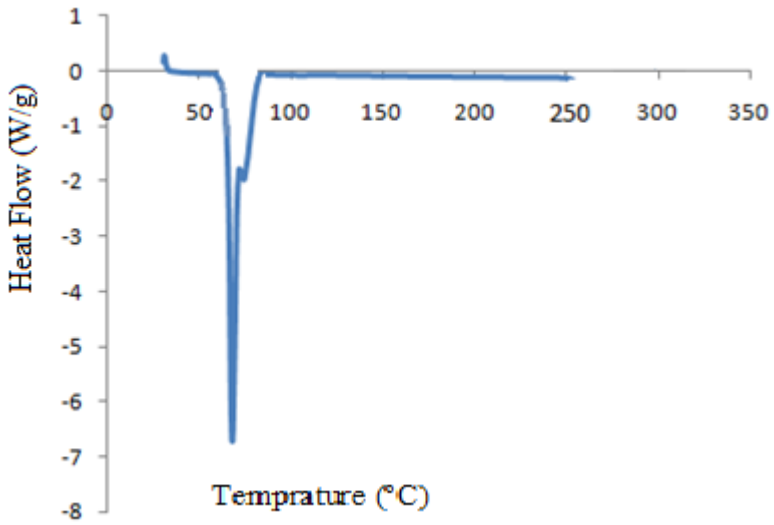

(A)

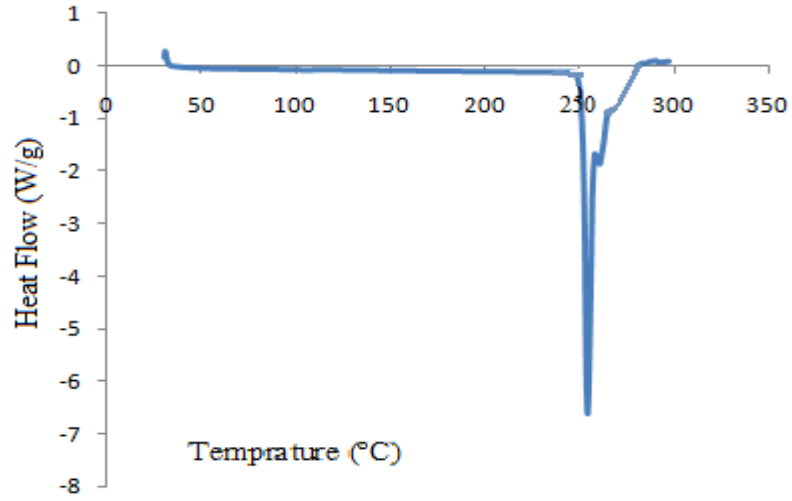

(B)

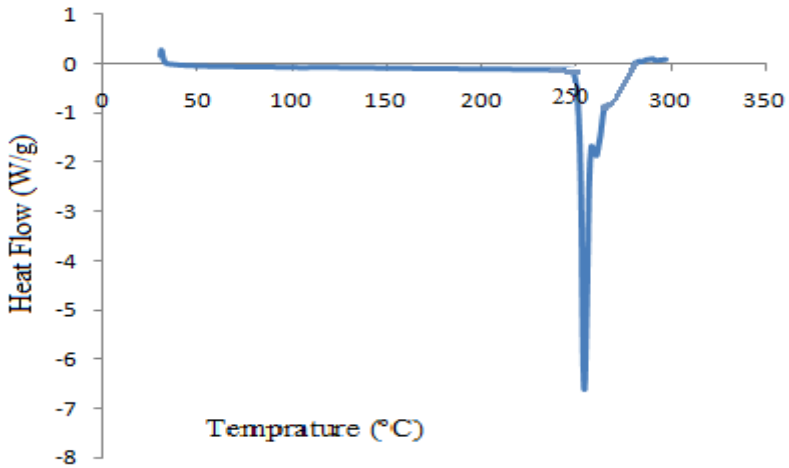

(C)

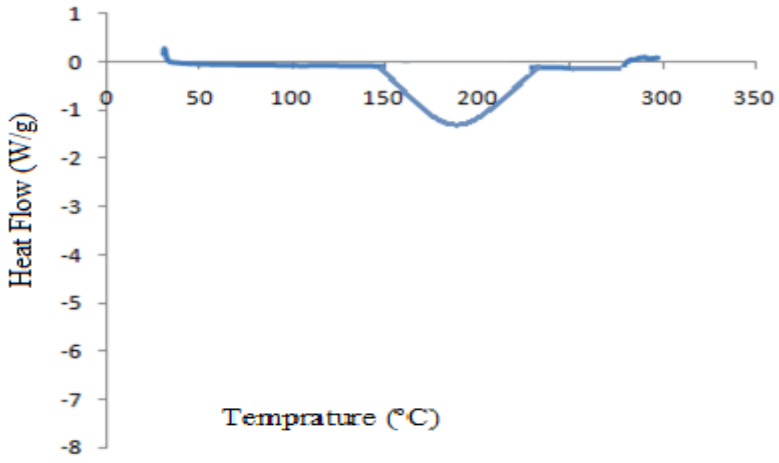

(D)

Figure 5.8: Differential scanning calorimetry (DSC) of (A) Gelatin; (B) Colchicine; (C) Folic acid; (D) Folic acid conjugate gelatin.

Particle size

The mean particle size of nanoparticles were determined to predict the in vitro and in vivo behavior of N. Dixit et al. / Biomedicine & Pharmacotherapy 69 (2015) 1–104 nanoformulation in physiological milieu. The mean particle size of optimized CLC-GNs-FA was significantly (Unpaired ‘‘t’’ test, $P < 0.05$) higher than CLC-GNs and measured to be 225±31.5 nm and 150±30 nm, show in figure 5.9(A-B).

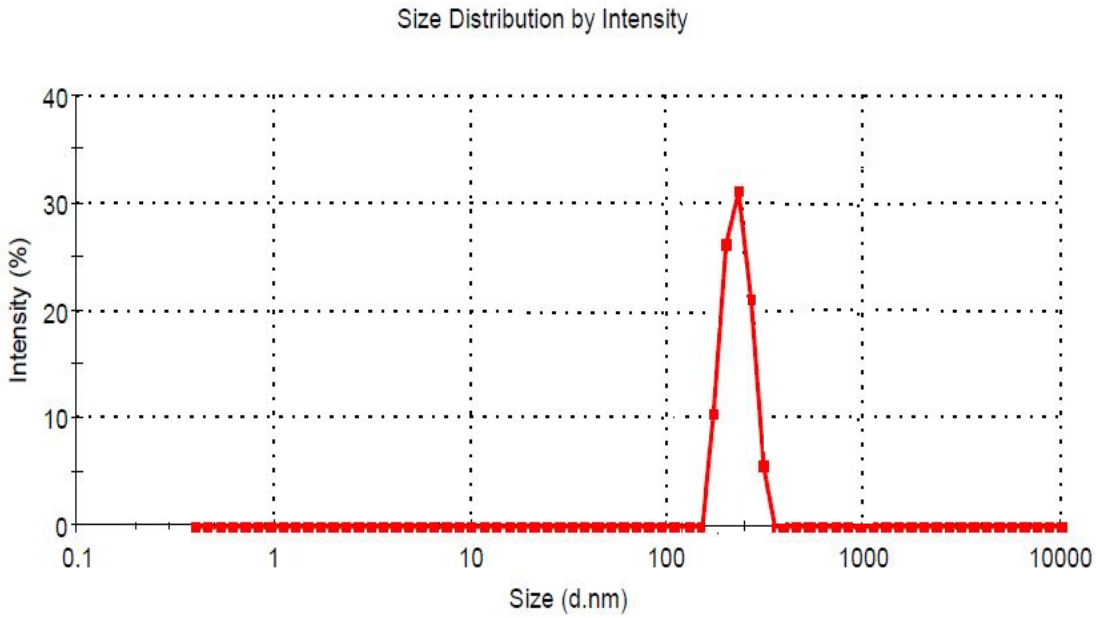

(A)

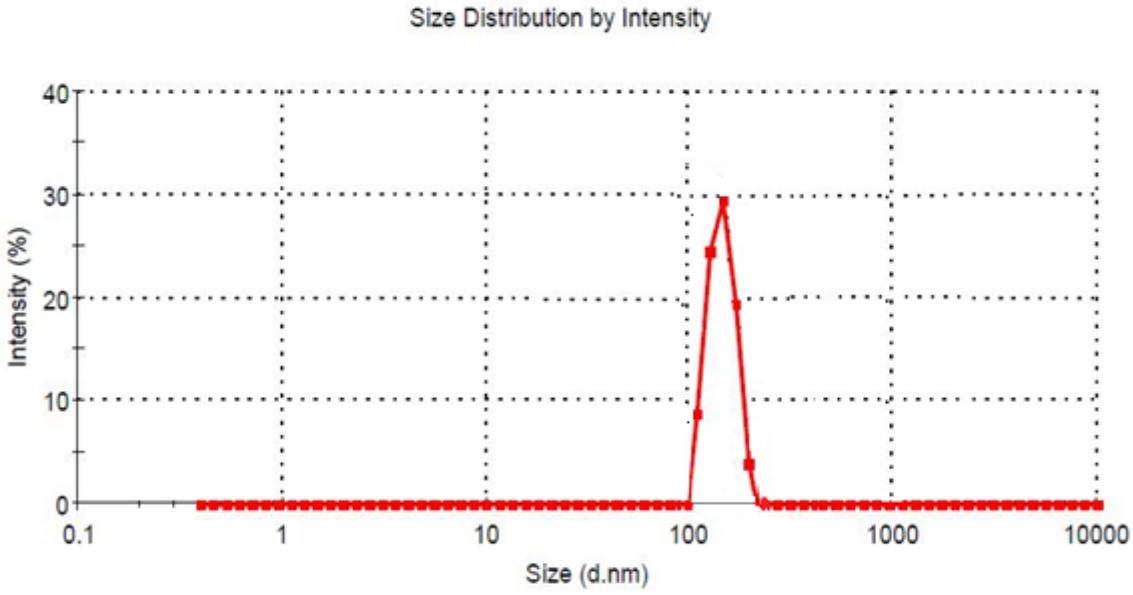

(B)

Figure 5.9: Particle size distribution of (A) Folic acid conjugated colchicine loaded gelatin nanoparticles, (B) Colchicine loaded gelatin nanoparticles.

Encapsulation

$$\text{Encapsulation efficiency} = \frac{\text{Amount of drug entrapped}}{\text{Amount of drug added}} \times 100$$

$$\text{Drug loading capacity} = \frac{\text{Amount of drug present}}{\text{Practical yield of nanoparticles}}$$

Percentage efficiency of CLC loaded gelatin nanoparticles was found to be 91.3±2.9% and percentage efficiency of folic acid conjugated CLC loaded gelatin nanoparticles was found to be 92.3±4.0%.

Table 5.3: Characterization parameters for colchicine loaded nanoparticles.

Sample	Particle size (nm)	Nanoencapsulatio Efficiency %	Drug loading capacity
CLC-GNs	150±30	91.3±2.9	7.5mg/10mgof nanoparticles
CLC-GNs-FA	225±31.5	92.3±4.0	8.1mg/10mg of nanoparticles

In-vitro drug release profile

In vitro release of colchicine from nanoparticles was analyzed by dynamic dialysis method in PBS of pH ~ 7.4 to simulate the cancer cell compartment and normal body physiology milieu. Release kinetic of a drug from the dialysis membrane depends on the permeability constant, which was measured by inserting 100 mg/mL of colchicine inside the dialysis bag followed by measuring the drug concentration in the receptor chamber (C1) as a function of time. Using the equation for permeability constant, KCV was calculated (0.052/h/mL). The intercepts on the axis gave the value of the original amount of colchicine present inside the dialysis membrane, which was approximately 99.8 mg, almost identical to the original amount showing that adsorption of the drug by the dialysis membrane was negligible. A representative graph of the release kinetics of colchicine from CLC-GNs and optimized CLC-GNs-FA is shown in Fig.5.10. Drug release was found to follow a first-order release kinetic at pH ~7.4 with characteristics of biphasic release. Release rate constants for two phases were given by the slopes. The CLC-GNs and optimized CLC-GNs-FA released 91.23% and 88.41 % of colchicine at pH~7.4, that were significantly (one-way ANOVA, $P < 0.05$) higher than the 75.3% and 70.5% of colchicine released by CLC-GNs and CLC-GNs-FA, respectively at pH~7.4.

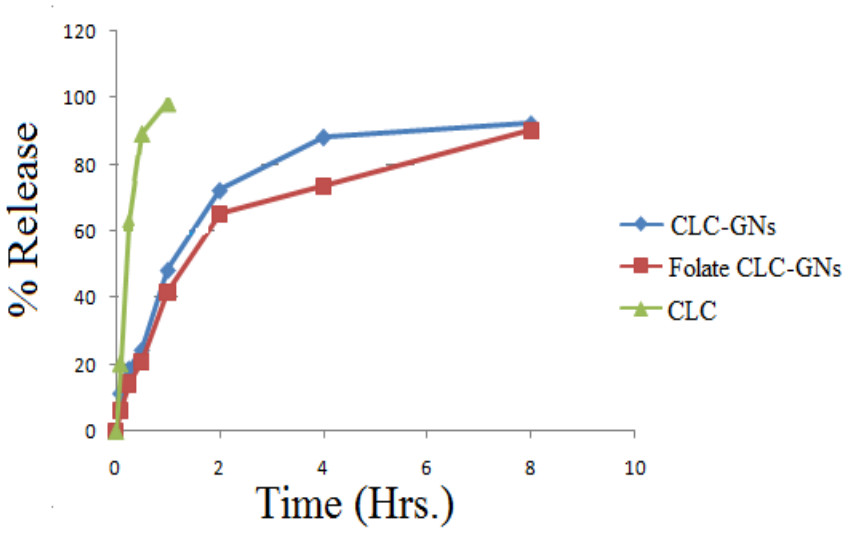

Figure 5.10: Release profile of colchicine loaded gelatin nanoparticles (Clc-GNs) and optimized colchicine loaded folate-grafted gelatin nanoparticles (CLC-GNs-FA) in phosphate buffer saline (pH~7.4). Optimized CLC-GNs-FA and CLC-GNs at pH~7.4 released 88.41% and 91.23% of colchicine, significantly (one-way ANOVA, P < 0.05) greater than 70.53% and 75.34% of the drug released at pH~7.4. The dissolution testing was carried out in triplicate (n≥3).

Cytotoxicity assay

IC_{50} – 30 µg/ml of CLC

IC_{50} - 25 µg/ml of CLC loaded GN-NPs

IC_{50} – 20 µg/ml of folate conjugated CLC loaded GN-NPs

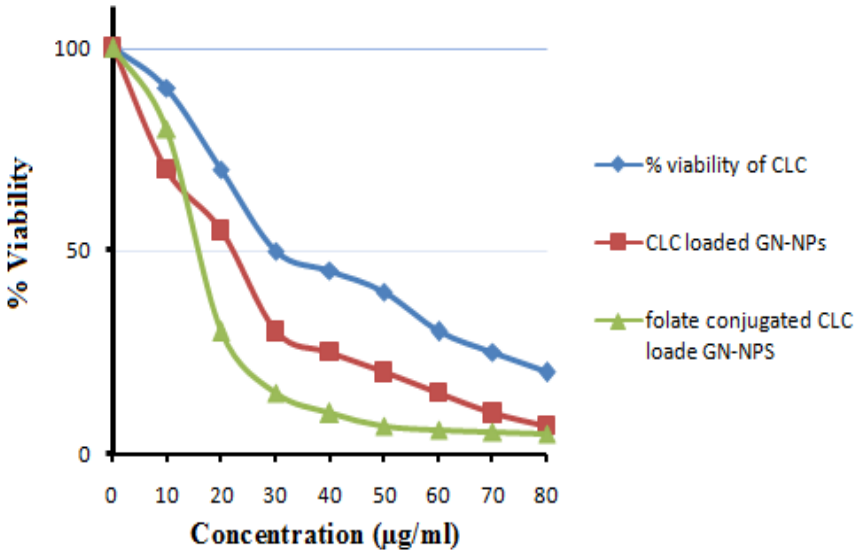

Figure 5.11: In-vitro cytotoxicity assay.

Cellular uptake assay

We determined quantitatively and qualitatively the accumula-tion of nanoparticles in MDA-MB-231 cells by trafficking FITC-labeled CLC- GNs and optimized CLC-GNs-FA using a fluorometer and CLSM (Spectra Fluor, Tecan, Switzerland). Both fluorescent nanoformulations were stable in cell culture medium, as determined by in vitro release of FITC from FITC-labeled CLC-GNs and optimized CLC-GNs-FA. We observed negligible, 2.5% and 3.1% release of FITC in FA-free-DMEM and PBS (pH~7.4) respectively, as compared to 34.5% in acetone in 24 h. Furthermore, optimized, CLC-GNs FA showed maximally ($P < 0.05$, two-way ANOVA) 80.54 ± 7.60% cellular accumulation as compared to 51.68 ± 9.78% by CLC-GNs in MDA-MB-231 scells, treated with a gradient concentration of nanoparticles at the concentration equivalent to 10–70 mM of cisplatin (fig 5.12). Consistent with the quantitative results, photo-micrographs of cellular uptake of optimized CLC-GNs-FA and CLC-GNs in MDA-MB-231 cells confirmed the qualitative analysis (fig 5.12). Optimized CLC-GNs-FA exhibited higher accumulation preferentially in the cytoplasm of MDA-MB-231 cells, therefore, depicted comparatively elevated fluorescence, as compared to CLC-GNs.

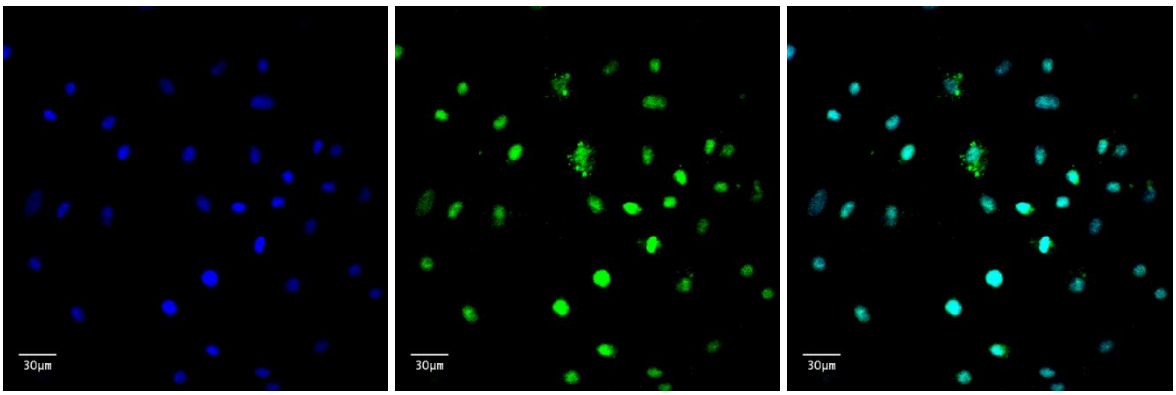

DAPI **FITC** **Merged**

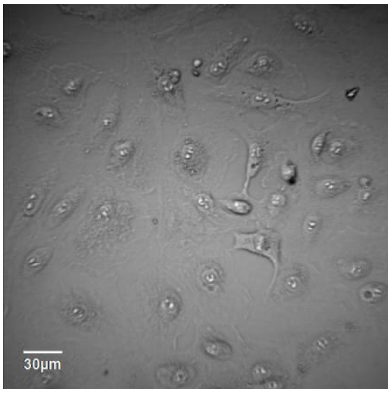

DIC

Figure 5.12: Cellular uptake analysis in breast cancer(MDA-MB-231) cells,(A) quantitative analysis indicated significantly (P < 0.05, two-way ANOVA) higher cellular accumulation (80.54~7.60%) by FITC-labeled optimized colchicine loaded folate-grafted gelatin nanoparticles (CLC-GNs-FA) as compared to 51.68~9.78% by colchicine loaded gelatin nanoparticles (CLC-GNs) expressed in terms of mean fluorescence intensity and percent cellular accumulation, Fluorescence value of nanoformulations at time '0 h' was designated as 100%. (B) Confocal laser-scanning microscope (CLSM) images of cellular uptake of FITC-labeled optimized CLC-GNs-FA that showed higher accumulation preferentially in the cytoplasm of MDA-MB-231 cells as compared to CLC-GNs. DAPI was used for nucleus staining. Nanoparticles are showing green color fluorescence. Scale bar ~20 µm.

CONCLUSION

Colchicine (CLC), an anticancer agent acts by de-stabilizing the cancer cells. However, its pharmacokinetics and pharmacodynamic properties are affected by low aqueous solubility and oral bioavailbility. We have synthesized ligand decorated nanoparticlesusing folic acid and gelatin for targeting breast cancer cells. Gelatin was successfully employed to prepare CLC loaded nanoparticles <200 nm using optimized two-step desolvation method. We have shown the optimization of CLC-FA-GNs for the efficient delivery CLC into brest cancer cells. Our systemic and methodological investigation of various synthesis parameters governing nanoparticles preparation showed that CLC-GNs and CLC-FA-GNs can be synthesized with a narrow particle size distribution. The prepared CLC-FA-GNs was evaluated by Fourier-transform infrared spectroscopy (FTIR), differential scanning calorimetry (DSC), powder X-ray diffractometry (PXRD), transmission electron microsopy (TEM). Therefore, we have presented here a CLC for the development of viable anticancer formulation. Further, in vitro cytotoxicity and cellular uptake study confirmed that CLC-FA-GNs with greater efficacy compared with CLC alone and CLC-GNs may potentially be used for targeting breast cancer cells.

REFERENCES

1. Baguley BC, Zhuang L, Kestell PIncreased plasma serotonin following treatment with flavone-8-acetic acid, 5, 6-dimethylxanthenone-4-acetic acid, vinblastine, and colchicine: relation to vascular effects, 1997; 9(2): 55-60.

2. Baguley BC, Holdaway KM, Thomsen LL, Zhuang L, Zwi LJ. Inhibition of growth of colon 38 adenocarcinoma by vinblastine and colchicine: evidence for a vascular mechanism. Eur J Cancer, 1991; 27(4): 482-7.
3. Yokoyama C, Yajima C, Machida T, Kawahito Y, Uchida M, Hisatomi H.Interleukin-8 enhances the effect of colchicine on cell death.Biochem Biophys Res Commun, 2017; 485(1): 89-94.
4. Fabresse N, Allard J, Sardaby M, Thompson A, Clutton RE, Eddleston M, Alvarez JC.LC-MS/MS quantification of free and Fab-bound colchicine in plasma, urine and organs following colchicine administration and colchicine-specific Fab fragments treatment in Göttingen minipigs.J Chromatogr B Analyt Technol Biomed Life Sci, 2017; 1060: 400-46.
5. Chang HY, Shih MH, Huang HC, Tsai SR, Juan HF, Lee SC,Middle infrared radiation induces G2/M cell cycle arrest in A549 lung cancer cells.PLoS One, 2013; 8(1): e54117.
6. Spasevska I, Ayoub AT, Winter P, Preto J, Wong GK, Dumontet C, Tuszynski JAModeling the Colchicum autumnale Tubulin and a Comparison of Its Interaction with Colchicineto Human Tubulin.Int J Mol Sci, 2017; 18(8).
7. Ruiz Gómez MJ, Gil L, Souviron A, Martínez Morillo M.Multidrug resistance increment in a human colon carcinoma cell line by colchicine,J Physiol Biochem, 2000; 56(1): 33-8.
8. Mangiatordi GF, Trisciuzzi D, Alberga D, Denora N, Iacobazzi RM, Gadaleta D, Catto M, Nicolotti O.Novel chemotypes targeting tubulin at the colchicine binding site and unbiasing P-glycoprotein,Eur J Med Chem, 2017; 139: 792-803.
9. Johnson L, Goping IS, Rieger A, Mane JY, Huzil T, Banerjee A, Luduena R, Hassani B, Winter P, Tuszynski JA, Novel Colchicine Derivatives and their Anti-cancer Activity, Curr Top Med Chem, 2017; 17(22): 2538-2558.
10. Lindamulage IK, Vu HY, Karthikeyan C, Knockleby J, Lee YF, Trivedi P, Lee H'Novel quinolone chalcones targeting colchicine-binding pocket kill multidrug-resistant cancercells by inhibiting tubulin activity and MRP1 function, Sci Rep, 2017; 7(1): 10298.
11. Balal M, Seyrek N, Karayaylali I, Paydaş S, Permanent improvement of renal dysfunction and proteinuria with colchicine in a patient with tumoral amyloidosis and basal cell carcinoma, Ren Fail, 2003; 25(4): 677-80.

12. Ruiz-Gómez MJ, Souviron A, Martínez-Morillo M, Gil L,P-glycoprotein, glutathione and glutathione S-transferase increase in a colon carcinoma cell line by colchicine,J Physiol Biochem, 2000; 56(4): 307-12.
13. Kumar A, Sharma PR, Mondhe DM, Potential anticancer role of colchicine-based derivatives: an overview, 2017; 28(3): 250-262.
14. Banks P, Mayor D, Mitchell M, Tomlinson D, Studies on the translocation of noradrenaline-containing vesicles in post-ganglionic sympathetic neurones in vitro. Inhibition of movement by colchicine and vinblastine and evidence for the involvement of axonal microtubules, J Physiol, 1971; 216(3): 625-39.
15. Aivaliotis M, Kontochristopoulos G, Hatziolou E, Aroni K, Zakopoulou N, Successful colchicine administration in facial granulomas caused by cosmetic implants: report of a case, J Dermatolog Treat, 2007; 18(2): 112-4.
16. Smith RL, Åstrand OA, Nguyen LM, Elvestrand T, Hagelin G, Solberg R, Johansen HT, Rongved P, Synthesis of a novel legumain-cleavable colchicine prodrug with cell-specific toxicity, Bioorg Med Chem, 2014; 22(13): 3309-15.
17. Wang RC, Chen X, Parissenti AM, Joy AA, Tuszynski J, Brindley DN, Wang Z, Sensitivity of docetaxel-resistant MCF-7 breast cancer cells to microtubule-destabilizing agents including vinca alkaloids and colchicine-site binding agents, PLoS One, 2017; 12(8): e0182400.
18. O'Brien TG, Simsiman RC, Boutwell RK, The effect of colchicine on the induction of ornithine decarboxylase by 12-O-tetradecanoyl-phorbol-13-acetate, Cancer Res, 1976; 36(10): 3766-70.
19. Charpentier MS, Whipple RA, Vitolo MI, Boggs AE, Slovic J, Thompson KN, Bhandary L, MartinSS, Curcumin targets breast cancer like cells with microtentacles that persist in mammospheres and promote reattachment, Cancer Res, 2014; 74(4): 1250-60.
20. Bhattacharyya B1, Panda D, Gupta S, Banerjee M.Anti-mitotic activity of colchicine and the structural basis for its interaction with tubulin.Med Res Rev, 2008; 28(1): 155-83.
21. Zhou J, Giannakakou P. Targeting microtubules for cancer chemotherapy. Curr Med Chem Anticancer Agents, 2005; 5(1): 65-71.
22. Tripathi KD. Chemotherapy of neoplastic disease. Essentials of medical pharmacology. Delhi: Jitender P Vij, 2003; 5: 769.
23. Jaiswal J, Gupta SK, Kreuter J. Preparation of biodegradable cyclosporine nanoparticles byhigh-pressure emulsifi cation solvent evaporation process. J Control Release, 2004; 96: 169–78.

24. Sterry W, Steigleder GK, Nikolai B. Elevated colchicine sensitivity of dermal lymphocytes in mycosis fungoides. Acta Derm Venereol, 1980; 60(3): 257-9.
25. E-shabouri MH. Positively charged nano particles for improving the oral bioavailability of cyclosporine-A. Int J Pharm, 2002; 249: 101–8.